Compact and Closely Spaced Tunable Printed F-Slot MIMO Antenna System for Portable Wireless Applications with Efficient Diversity

I.T.E. Elfergani, A.S. Hussaini, N. A. Jan, C.H. See, R.A. Abd-Alhameed, S. Zhu, J.Rodriguez and N.J. McEwan

Abstract

In this work, miniaturized tunable two-antenna MIMO systems composed of printed F-slot shaped is developed to operate in the GPS, PCS, DCS and UMTS bands. The two-element MIMO antenna occupies a volume of 50 × 37.5 ×1.6 mm^3, and is printed on an FR4 substrate. Initially, the frequency tunability of the MIMO antennas was verified by lumped capacitors with values between 0.75 to 2.75 pF to achieve a tuning range from 1.55 to 2.07GHz while the low mutual coupling between the radiators was accomplished by adding an I-shaped branch to a cut-away ground plane. The two antennas are then loaded with varactors to simultaneously achieve miniaturization and tunability. Simulation and measurement results demonstrate the successful implementation of a tunable MIMO with coupling reduction mechanism for a portable handheld wireless transceiver. The channel capacity of the proposed antenna is investigated and found to be close to that of an un-correlated system with efficient diversity in which the mutual coupling across the full

bandwidth was better than -13dB. Owing to the compact size and ease of manufacture, the proposed antennas can be a promising solution for adaptive MIMO systems in handheld devices.

Index Terms— multiple- input multiple-output (MIMO), tunable antenna, varactor diode, GPS, DCS, PCS, UMTS.

1. INTRODUCTION

The next generation of high bit-rate wireless communications will exploit the advantages of reduced multipath fading and increased channel capacity inherent in multiple-input-multiple-output (MIMO) RF architectures. MIMO techniques are already present in 4G wireless systems. Their use increases the communication throughput by using multiple antennas at the transmit and receive terminals. The design of MIMO antenna systems for handheld devices poses a serious challenge for antenna designers due to the physical space requirements. In the literature, several antenna structures are used for MIMO applications [1-30]. In general, various planar types have been used, including planar inverted F-type antennas (PIFA); a dual-element PIFA operating at 2.5 GHz is discussed in [1]. Attributes such as small size, low cost and ease of manufacture of printed monopole antennas motivate its application [2]. One advantage of the printed monopole antenna is the inherently omni-directional pattern for achieving maximum channel capacity [3]. Rapid developments in the use of MIMO systems in wireless communication demand novel antenna designs that can be used in more than one frequency band. The design of two back-to-back monopole antennas connected with a T-shaped stub for 2.4/5.2/5.8 GHz WLAN and 2.5/3.5/5.5 GHz WiMAX applications is presented in [4]. A tri-band E-shaped printed monopole antenna loaded with two U-shaped resonance paths suitable for MIMO systems for WLAN application, covering 2.4, 5.4, and 5.8 GHz is reported in [5].

It is more challenging for engineers to design a MIMO antenna for handset applications than for the base station, mainly due to the need for miniaturization and the mutual coupling that exists between the element antennas [6,7]. Indeed, in the latter, it is difficult to pack multiple antennas elements closely within the confines of a mobile handset whilst maintaining good isolation since the antennas are strongly coupled with each other and share a common ground and near field coupling [8]. Their pattern correlation coefficient is directly related to the coupling and a low value increases the achievable transmission speeds [9]. Many studies have been carried out to reduce coupling between multiple antenna elements. A corrugated ground plane with $\lambda/4$ slot was used to reduce the interference of a current flowing in the common ground plane [10]. In [11-12], a protruding T-shaped stub and L shaped stub at the ground plane are used to reduce coupling between two antennas. It is also interesting to note that by adding a lumped-element decoupling network after the two coupled antenna, inter-port isolation better than 15 dB can be obtained for two planar radiators separated by 0.069λ [13]. However, this method will incur a slight increase in manufacturing costs and any losses in the lumped elements will impair the radiation efficiency of the antenna.

Many efforts have been made using electromagnetic band gap (EBG) structures [14-18] to suppress the unwanted surface propagating wave at a specific frequency, and thus minimize the inter-element coupling. These EBG structures provide substantial decoupling but suffer from large surface area, high cost of manufacturing and complicated design. To avoid increasing the volume and weight of the antenna, authors in [19-23] propose a neutralization technique to cancel out the reactive coupling between two closely placed radiators. This is done by physically connecting the multiple antenna elements with a transmission line. This method has been initially used on a suspended PIFA antenna structure as in [19-20], and was

further adopted in a printed microstrip antenna array for mobile applications [21]. The results in [19]–[21] show that this technique provides an isolation of about 18 dB between two antenna elements. Other meta-material inspired solutions offer further choices to mitigate mutual coupling [24]. This technology has the advantage of reducing the circuit size whilst providing equivalent or better performance in both antenna and passive circuit applications.

However, all these methods [1-24] are only capable of offering fixed frequency bands and cannot be altered once fabricated. The smart handsets for emerging markets operate at multiple frequency bands and require a relatively large antenna footprint. They employ more than one radiating element to support multiple wireless functions or provide the diversity needed in a MIMO technology. Adopting tunable antenna designs is a viable solution to overcoming bandwidth limitations set by antenna size (the Chu-Harrington limit) [25], and to compensating for the loading effect of the deployment environment. A practical design objective in implementing tunable antennas is to achieve adequate tuning range and tuning resolution across as many channels as possible, though tuning resolution is not a problem for continuously variable tuning elements such as varactors. Recently, a reconfigurable antenna array has been used in an adaptive MIMO system to further exploit the theoretical performance of MIMO systems [26-29]. Such a system is capable of changing the radiation properties of the antenna elements, depending on real channel responses, so that its performance can be optimized. However, to realize a reconfigurable antenna in a wireless device, especially in a mobile device, presents difficult challenges due to limitations of product volume and manufacturing cost. For MIMO systems, mutual coupling is a new and important parameter that has to be considered with traditional parameters, such as gain, radiation pattern, radiation efficiency and reflection coefficients, in achieving high performance of the antenna system.

A natural approach to achieve low mutual coupling is to physically separate the antennas [30 -33], which of course is barely possible for MIMO systems implemented in a handset that needs to be ergonomically small and slim. Thus, in this paper, a MIMO antenna with two tunable closely spaced monopole antennas is proposed. The antenna system discussed in this paper is based on the tuned structure proposed by the authors in [34-35]. The design presented here is essentially a feasibility study for a compact printed MIMO antenna system suitable for mobile tracking and wireless sensor applications, and with an acceptable mutual coupling (below −13 dB).

2. THE ANTENNA DESIGN CONCEPT

Fig. 1a shows the geometry of the proposed two-monopole MIMO antenna system formed on a single layer of low cost FR-4 material with thickness 1.6 mm, dielectric constant 4.4, and of loss tangent 0.02. The size of the system PCB selected in this study is 37.5 mm × 50 mm, which can represent the circuit board of a wireless terminal. The two monopoles are printed on the two opposite corners of the PCB (shown in the top portion of Fig. 1(a)). There are only a few areas where the antennas can be positioned under restrictions imposed by mobile phone manufacturers and this is usually on the top edge of the PCB [35]. Considering this constraint, we simulated and realized several two monopole configurations located in close proximity to each other. During analysis of the mutual coupling, the radiator's dimensions remained fixed; only the distance between the elements and the back protruded strip was adjusted to maintain a low coupling. The distance between the two monopole antennas was chosen to be 1.5mm (equivalent to 0.012 λ at the maximum achievable tuning frequency). The monopole radiating element consists of a rectangular F-slot patch. The dimension of the

rectangular patch is 15 × 18 mm^2. Each monopole is designed in a clearance area, i.e. where the ground plane is removed. The two monopoles are mirror images and symmetrically placed with respect to the PCB centre line as shown in Fig. 1(a). A 50 ohm microstrip (with dimensions 17.0 × 1.5mm^2) is used to feed each monopole antenna, which is also printed on the top layer of the substrate. Good impedance matching can be obtained without any other matching circuit. Figs. 1b and 1c show the bottom layers of the possible ground layers proposed in this work. The layout of the antenna with varactors and passive components is depicted in Fig. 1d and a simplified circuit diagram over the antenna geometry for one of the varactors diodes is presented in Fig. 1e which shows the flow of the D.C. bias applied in this design. This design has functional similarities with the single antenna application detailed in a prior investigation [34, 35], the MIMO operation being achieved by the duplicated structure. The main ground plane of the MIMO antenna is about 35 × 37.5mm^2 and there is an I-shaped branch extending from it and between the two monopole antennas. Both the I-shaped branch and the main ground plane are printed on the bottom layer of the substrate. The dimensions of the branch are 1.5× 15 mm^2, having been properly selected to obtain a high isolation. The preferred dimensions for antenna along with the I-shaped branch were obtained with the aid of the commercial simulator HFSS [36]. The cut-away ground structure is used to improve the impedance matching of the antenna as previously proposed by the authors in [34-35]. The mutual coupling between the proposed closely spaced antennas mainly comes from the induced current due to the sharing of the common ground and near field coupling.

To achieve sufficient isolation between the two identical elements and to maintain a good impedance matching over the desired frequency band, an I-shaped branch is introduced in this study. In principle, its function is to introduce an opposite coupling to reduce the mutual

coupling. Hence, the existing electromagnetic coupling between two antenna elements can be weakened. To find optimal locations of the I-shaped branch, several simulations were performed to check the isolation, return loss and radiation characteristics of the antenna. It was interesting to find these findings were in agreement with published works [11, 37, 38].

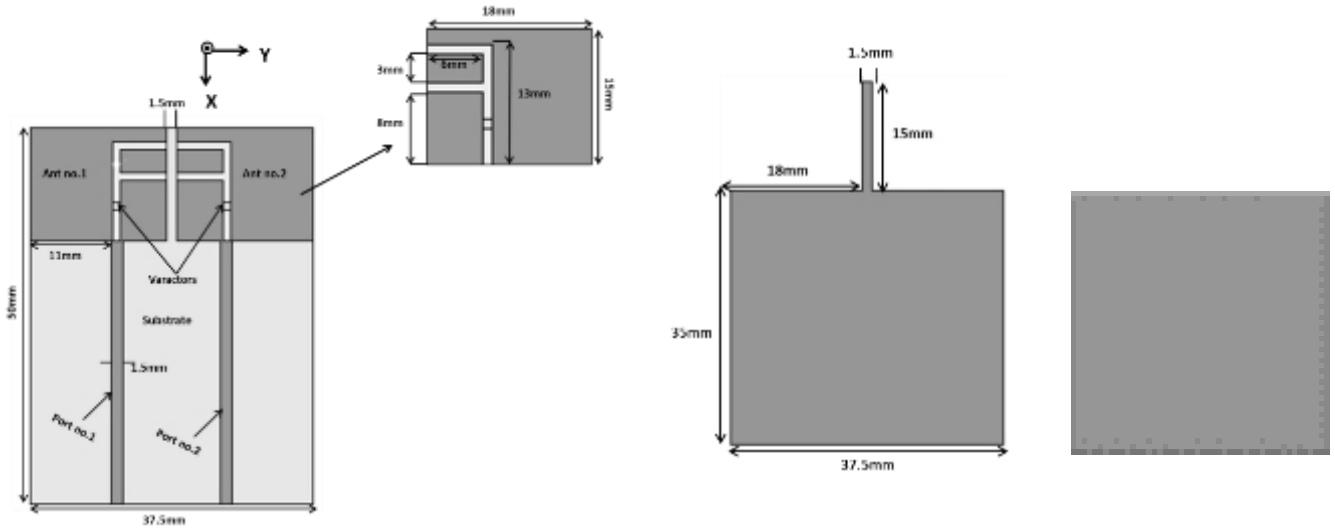

(a) (b) (c)

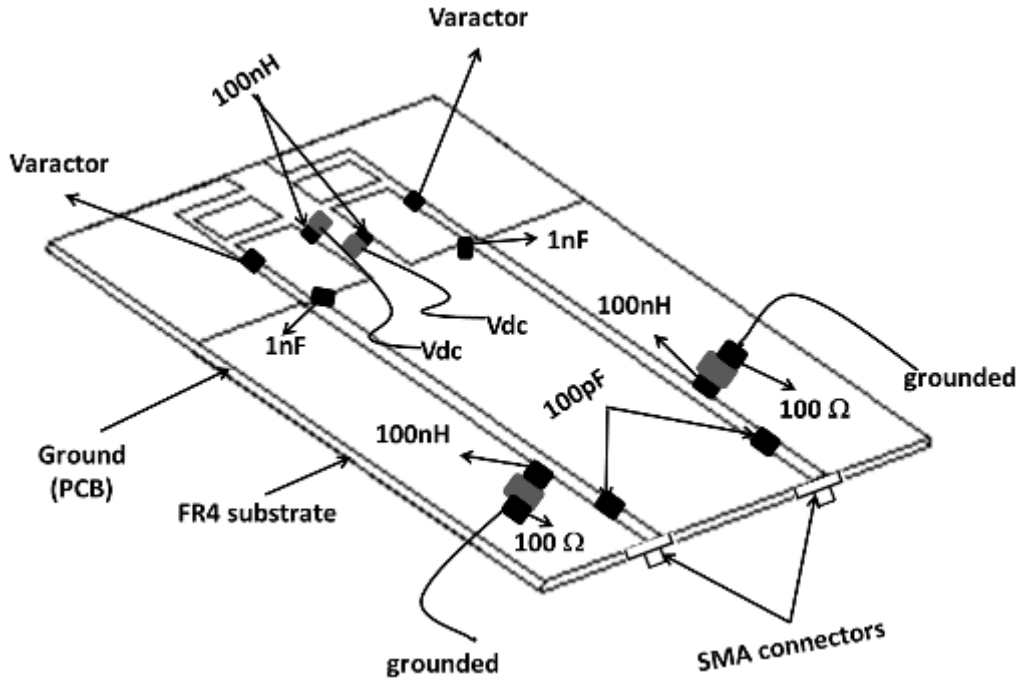

(d)

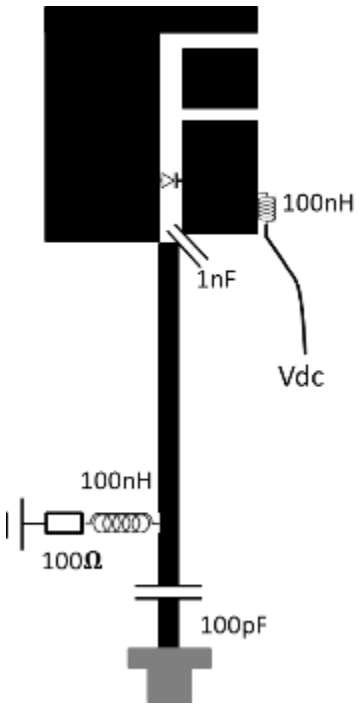

(e)

Figure 1: Geometry of Proposed antenna, (a) Top view, (b) ground with I-shaped branch, (c) ground without I-shaped branch, (d) 3D Schematic view of the proposed antenna with DC bias circuit, (e) A simplified equivalent DC bias circuit for one of the varactor diodes.

To evaluate the effectiveness of the I-shaped branch, the simulated reflection coefficient (S_{11}) and mutual coupling (S_{21}) of the proposed unloaded antenna with and without the line are shown in Fig. 2a. Due to the symmetrical structure, only S_{11} and S_{21} are represented. As can be seen, by introducing I-shaped branch onto the ground plane, the effect of reducing the mutual coupling to approximately -13 dB, whilst leaving the resonant frequency unaltered.

To further explain how the I-shaped ground branch reduces the mutual coupling, the surface current distribution of unloaded structure at the resonant frequency of 2.2GHz is shown in Fig. 2b. The surface current distribution on the entire element without the I-shaped branch

when input port of the antenna 1 is excited and input port of antenna 2 is terminated by 50Ω load, was demonstrated. In this case, the induced surface current on the antenna 2 is strong, so the mutual coupling is high. When the I-shaped branch is added to the ground plate, the induced surface current on antenna 2 is much weaker when the same excitation was applied, so the mutual coupling is much lower. The reason is that, antenna 1 induces coupling current on the I-shaped branch and antenna 2, respectively, and the I-shaped branch also induces coupling current on the antenna 2 where the two induced coupling currents on the antenna 2 are reversed, so the isolation is strengthened.

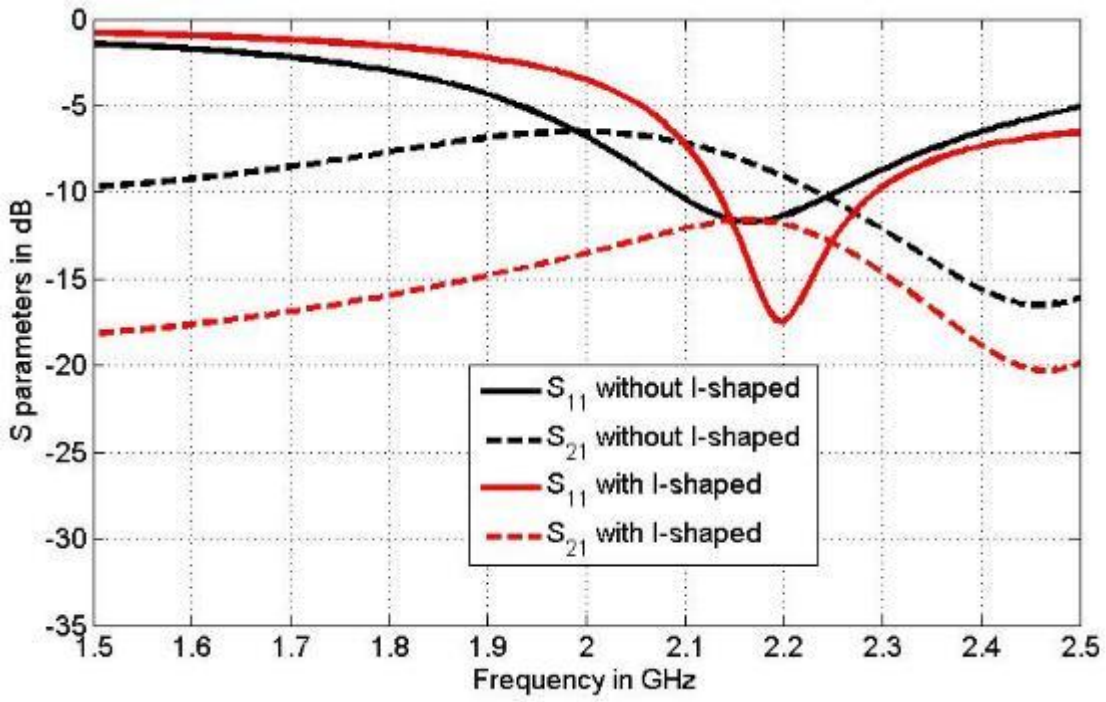

(a)

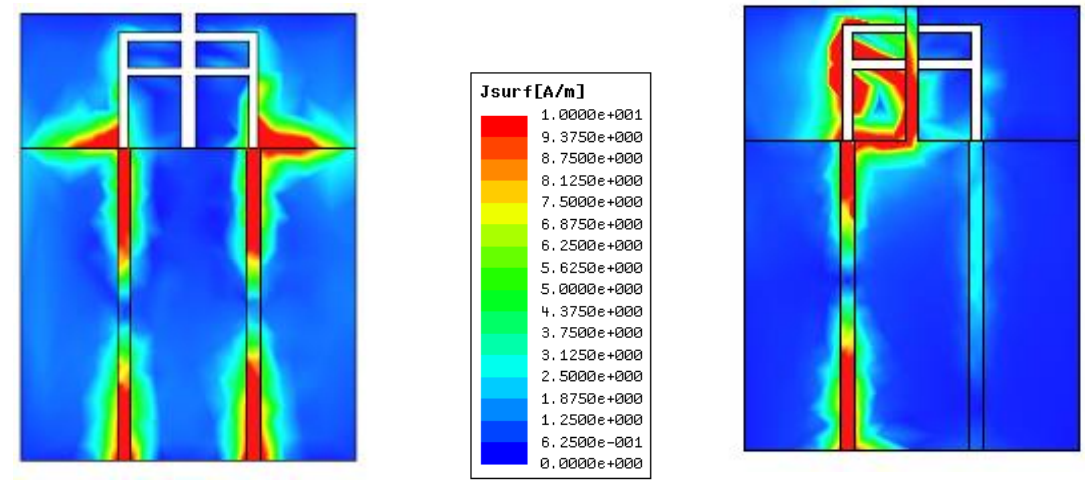

(top view)

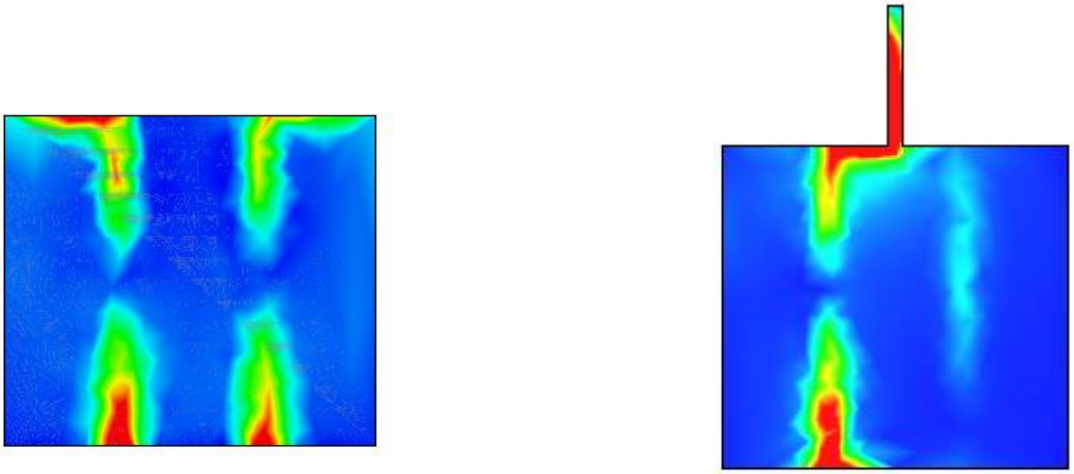

(bottom view)

(b)

Figure 2: Simulated S parameters of unloaded MIMO antenna with and without I-shaped branch (a) , Surface current distributions of unloaded antenna without I-shaped branch (*left*) and with (*right*) at 2.22GHz; Port 1 (*left*) is excited and port 2 is terminated by 50Ω (b).

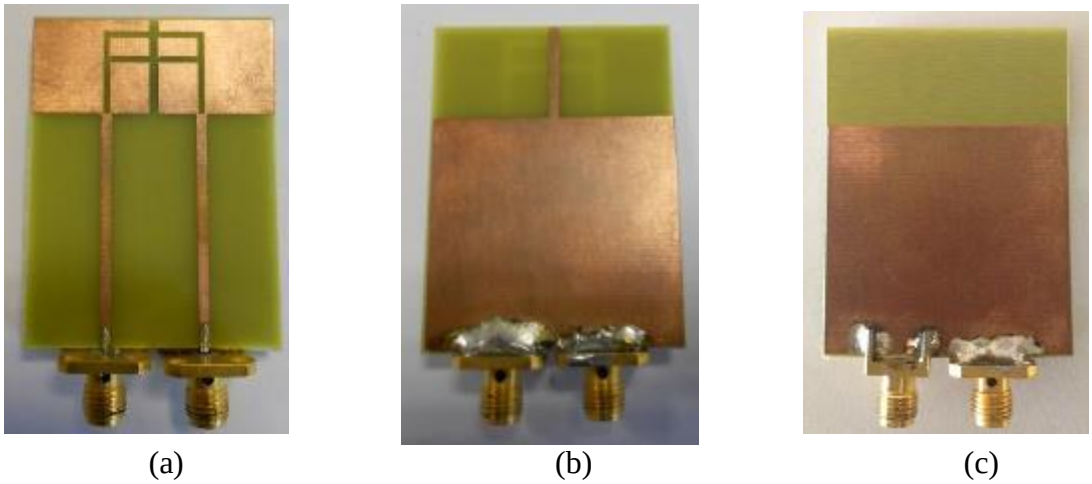

(a) (b) (c)

Figure 3: Prototype of unloaded antenna, (a) Top view, (b) ground with I-shaped branch, (c) ground I-shaped branch.

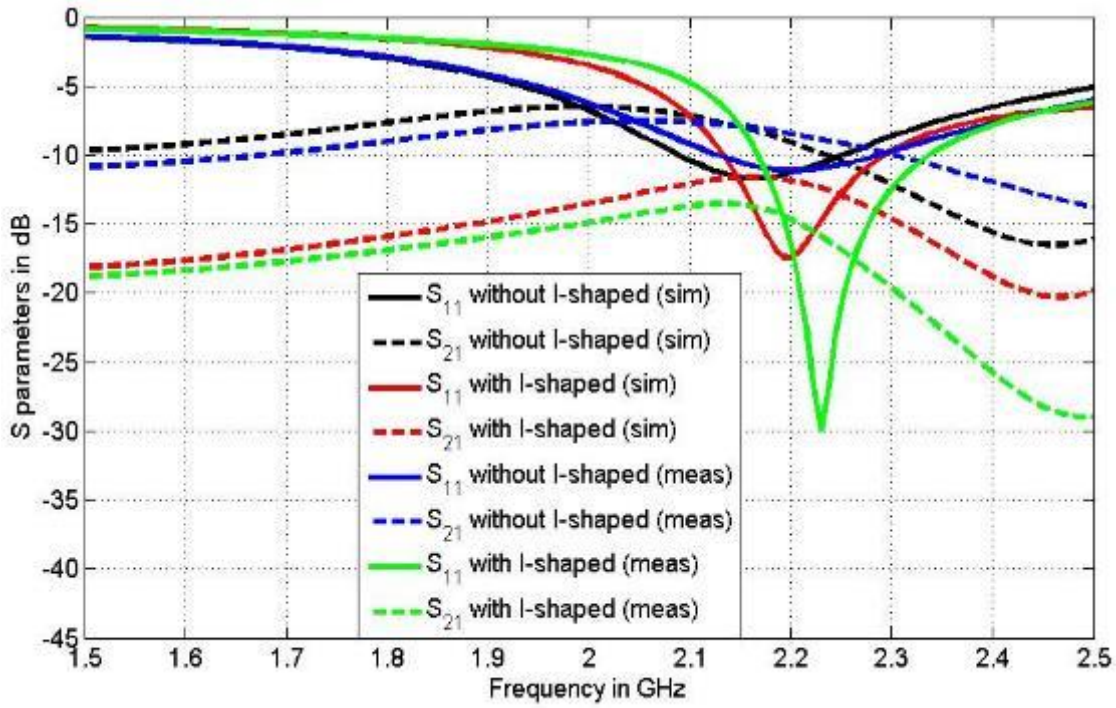

Figure 4: Measured S parameters of unloaded MIMO antenna with and without I-shaped branch

3. RESULTS AND DISCUSSION

To validate the simulated reflection coefficient results of the unloaded antenna system, a prototype of the proposed unloaded antenna as shown in Fig. 3 was first constructed and measured based upon on the design and dimensions as described in Fig. 1. Fig. 4 shows the measured reflection coefficients S_{11} along with their simulated counterparts, which are given in Fig. 2 (it should be noted that $S_{11} = S_{22}$ for symmetrical structure), and the isolation S_{21} between the two monopoles. As can be seen, the experimental data agrees with the simulation results. The measured impedance matching of the two monopoles over the 2.2 GHz band is below -10dB return loss, that is equivalent to VSWR ≤ 2. The isolation between the antennas was found below 13 dB. It is observed that without the I-shaped branch (the reference design, see Fig. 3), the antenna port isolation rapidly deteriorates by about 8 dB as seen in Fig. 4. This behaviour suggests that, by strengthening the isolation, an I-shaped ground branch with proper dimensioning may be used to generate an additional coupling path to lower the mutual coupling (below −13 dB).

The next phase of this work is the antenna tuning mechanism, which relies on the introduction of a varactor over the slotted radiator patch, which was derived from the HFSS model. For proper realization, this tuning requires the addition of two varactor diodes fixed at locations over the F-slots of both radiators along with passive components (see Figure 1(d)). The target tuning range is obtained by setting the same capacitance values from 0.75pF to

2.75pF over antenna element 1 and antenna element 2. Fig. 5 shows the simulated scattering parameters (S_{11}, S_{21}) for the loaded antennas without the I-shaped branch on the ground plane. It should be noted that without the I-shaped Branch present on the ground plane the effect of this capacitive loading cause the radiators to resonate over a wide frequency range from 1.55GHz to 2.07 GHz covering the GPS, PCS, DCS and UMTS bands, and moreover satisfy the impedance matching bandwidth requirement of $S11 < -10$ dB, with the mutual coupling being approximately -8 dB.

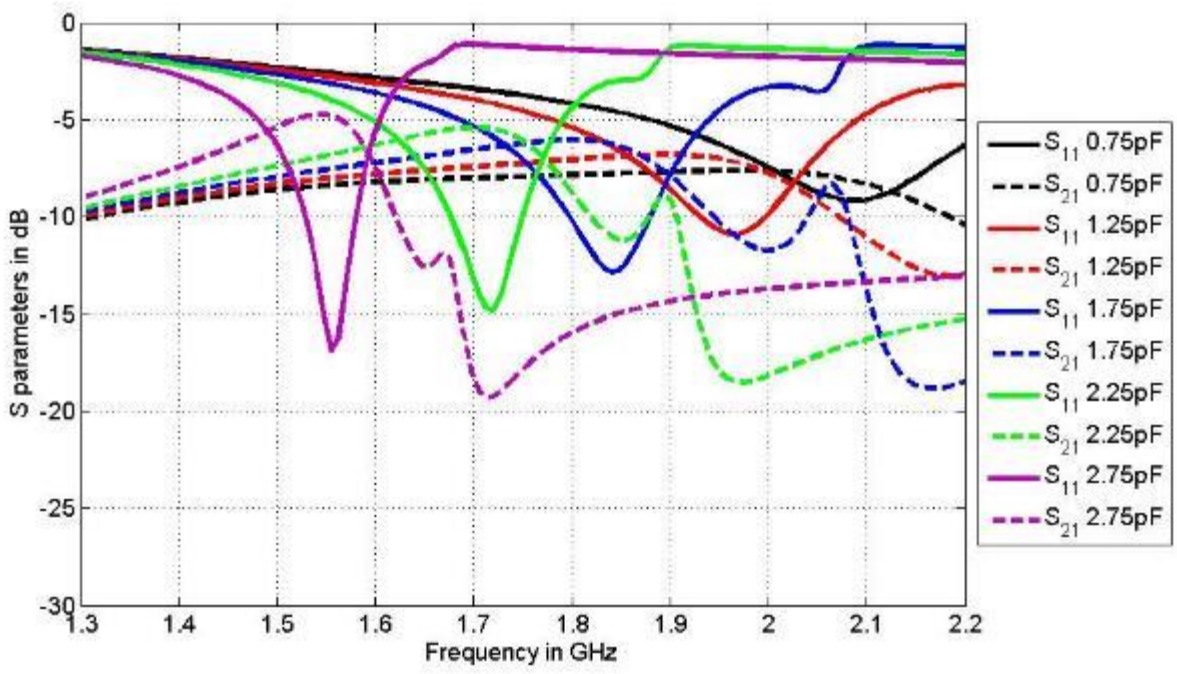

Figure 5: Simulated S parameters of loaded MIMO antenna without I-shaped branch

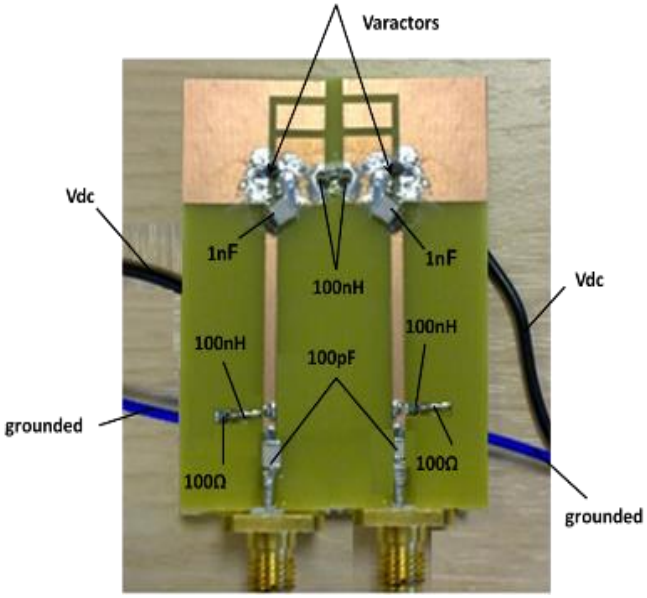

(a)

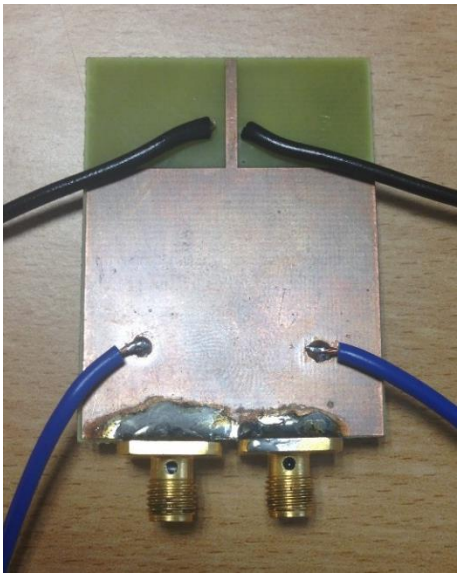

(b)

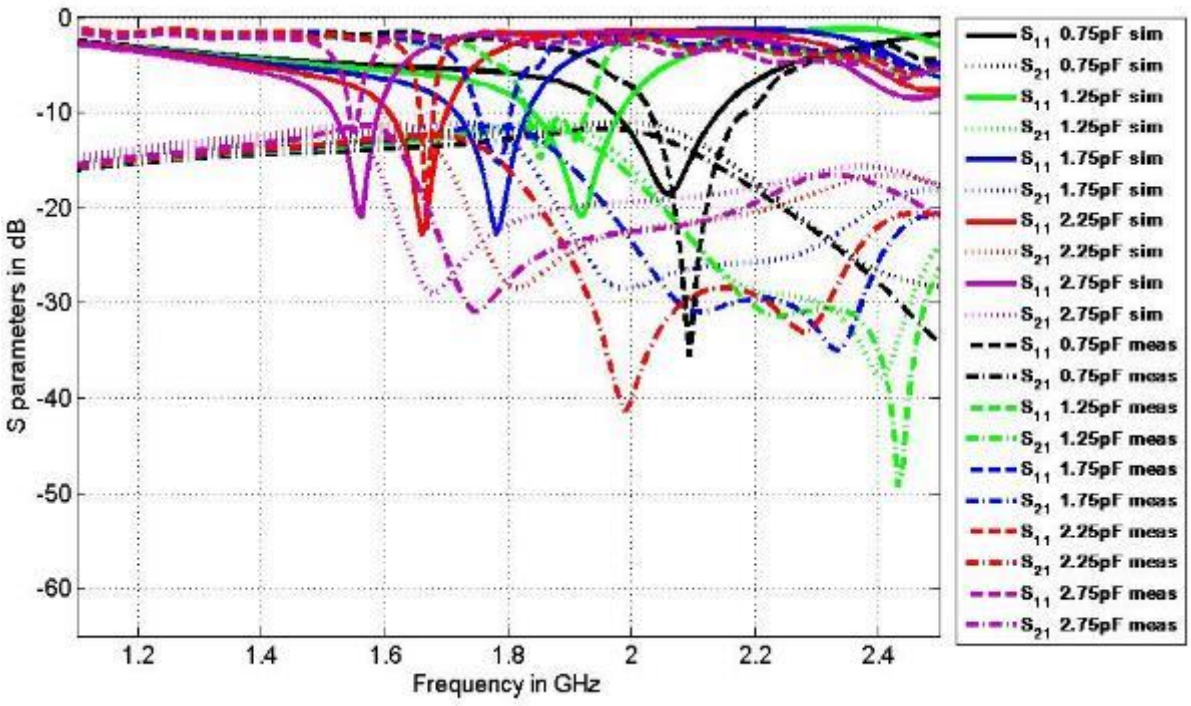

(c)

Figure 6: Prototype of loaded antenna with DC bias circuit, (a) Top view, (b) bottom view, (c) Simulated and Measured S parameters of loaded MIMO antenna with I-shaped branch

For-proof-of-concept, the antenna prototype including the I-shaped branch present on the ground plane along with tuning circuit are depicted in Fig. 6a and 6b. Two varactor diode packages (MMBV3102) with tuning circuits were used to achieve the tuning capability. The proposed antenna design along with these two varactor diodes, and passive components, are shown in Fig. 6a. As can be seen, for each antenna element, capacitor value of 100 pF was used to allow the RF signal to pass and block DC, while the second capacitor value of 1nF was used to avoid the shorting as shown in the patch. Two 100 nH RF chokes were used for DC passing. A 100 Ω resistor was used to control the current flowing to the varactor. The same frequency range from 1.55GHz to 2.07GHz was accomplished, but an opposite coupling is introduced due to the presence of the I-shaped branch on the ground plane which in turn reduces or improves the mutual coupling between the two element antennas. The simulated and measured values of S_{11} and S_{21} are plotted in Fig. 6(c), these results exhibit reasonable agreement with the simulated results computed by HFSS. It is noticeable that some discrepancies in simulated and measured result which can be attributed to : 1) fabrication tolerances in antenna; 2) some uncertainty in the electrical properties of substrate material; 3) accuracy of the simulation model for the varactor; 4) use of an ideal model for the resistor in simulation; 5) cable and SMA connector effects. However, both results clearly show that the impedance bandwidth of the antenna encompasses the operating frequency spectra from 1.55 to 2.07 GHz for a reflection coefficient for $S_{11} < -10$ dB while keeping the mutual coupling at the acceptable level ($S_{21} < -13$ dB) over the usable bandwidth.

Figure 7

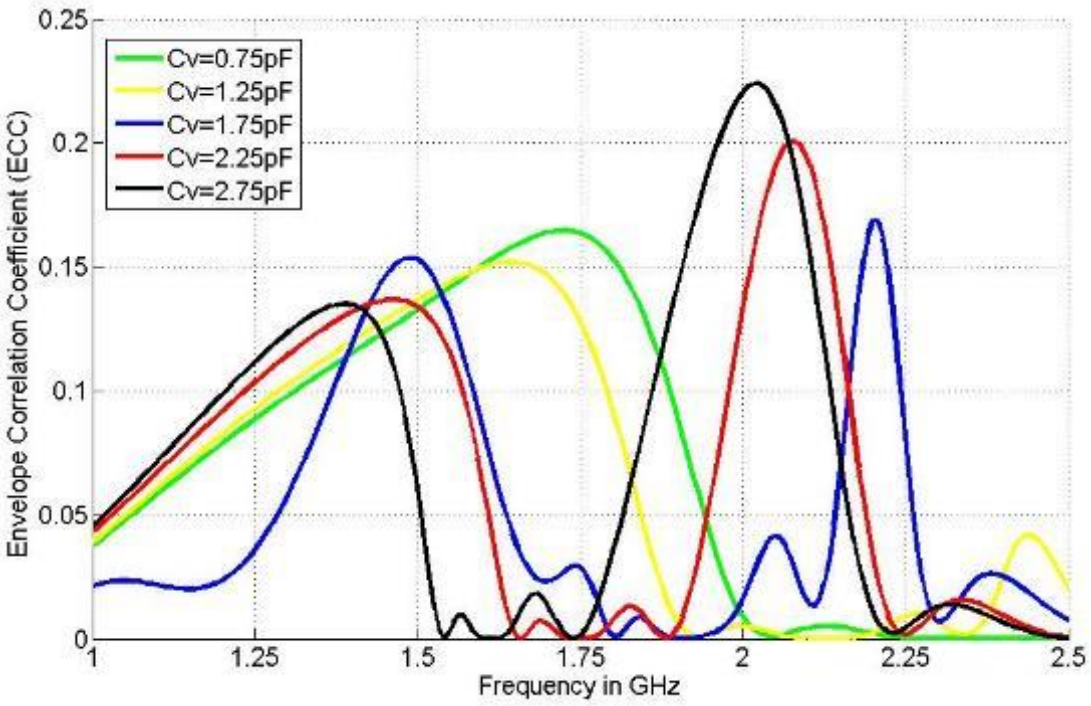

(a)

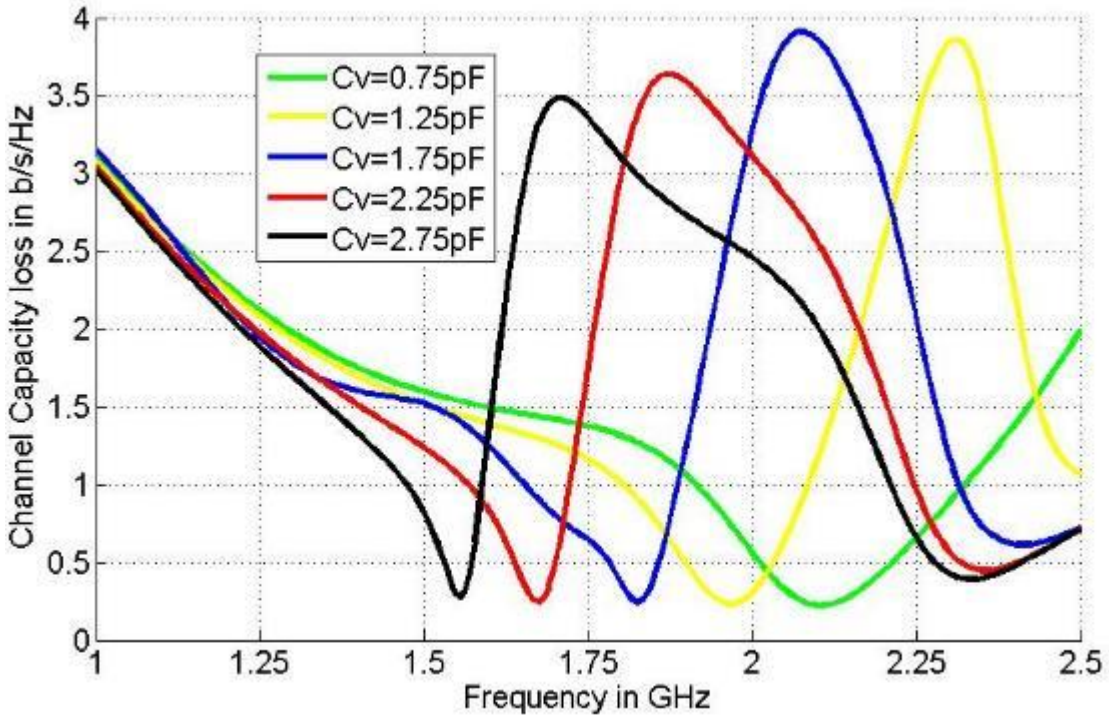

(b)

Figure 7: MIMO Characteristics of the antenna, (a) Correlation coefficient, (b) Capacity loss

For diversity in the proposed MIMO system, the correlation between signals received at the same side of a wireless link by the distinct antennas is an important figure of merit for the whole system. Commonly, the envelope correlation coefficient (ECC) is used to evaluate the diversity capability of a multi-antenna system. This parameter should preferably be computed from 3D radiation patterns [39], but this method is laborious. Assuming that a multiple antenna operates in a uniform multipath environment, its ECC can alternatively be [40]:

$$\rho_e = \frac{|S_{11}^* S_{12} + S_{21}^* S_{22}|^2}{(1-|S_{11}|^2 - |S_{21}|^2)(1-|S_{22}|^2 - |S_{12}|^2)} \quad (1)$$

To evaluate the performance of the MIMO antenna, the calculated ECC curve is shown in Fig.7a. It should be noted that the ECC of the two element antenna is always below 0.01 over the whole frequency band, which is comparable to the results obtained from [5], [19]. This is good indicator for promising diversity performance.

In theory, the channel capacity can be enhanced by increasing the number of antennas of the MIMO system. Nevertheless, the presence of Rayleigh-fading MIMO channels will induce loss of channel capacity. This loss can be calculated from the correlation matrices given in [41], [42]. In the case of a 2×2 MIMO system, assuming that only the receiving antenna patterns are correlated and assuming the worst scenario where high SNR is occurring, the capacity loss C_{loss} can be evaluated by using the following equation [40], [41]:

$$C_{loss} = log_2\, det(\psi^R) \quad (2)$$

where ψ^R is the receiving antenna correlation matrix that is given by:

$$\psi^R = \begin{bmatrix} \rho_{11} & \rho_{12} \\ \rho_{21} & \rho_{22} \end{bmatrix}, \rho_{ii=} 1 - (|S_{ii}|^2 + |S_{ij}|^2), \text{ and } \rho_{ij=-}(S_{ii}^* S_{ij} + S_{ji}^* S_{jj}), \text{ for } i, j = 1 \text{ or } 2 \quad (3)$$

The capacity losses of the proposed MIMO antenna are shown in Fig. 7b, where it can be seen that neither exceeds 0.25 bps/Hz over the targeted operating frequency band in which approves that good impedance matching and isolation between two antennas elements lead to low capacity loss. The ECC and channel loss along with bandwidth for each capacitor value is detailed in Table I.

Figure 8

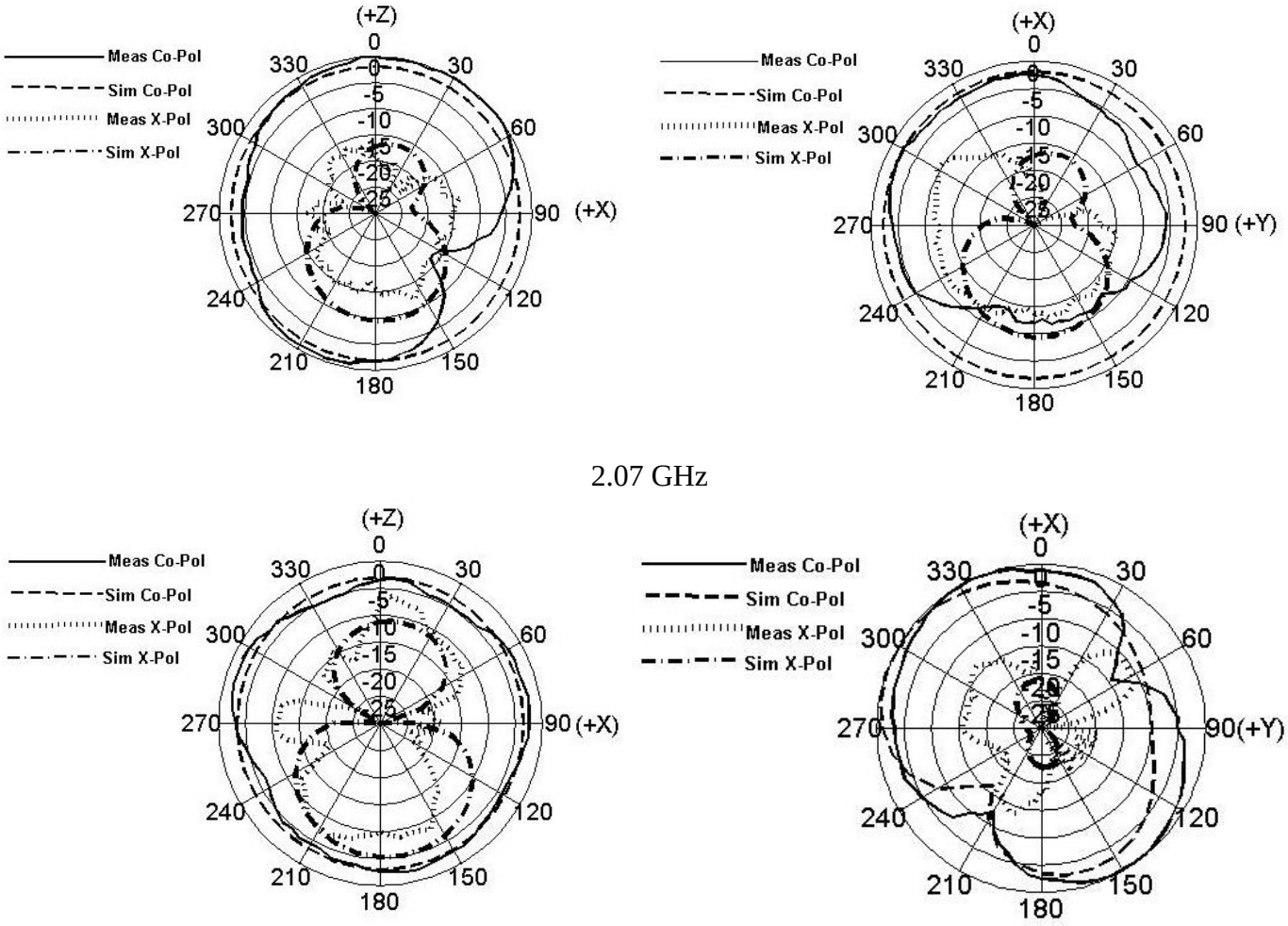

2.07 GHz

1.9 GHz

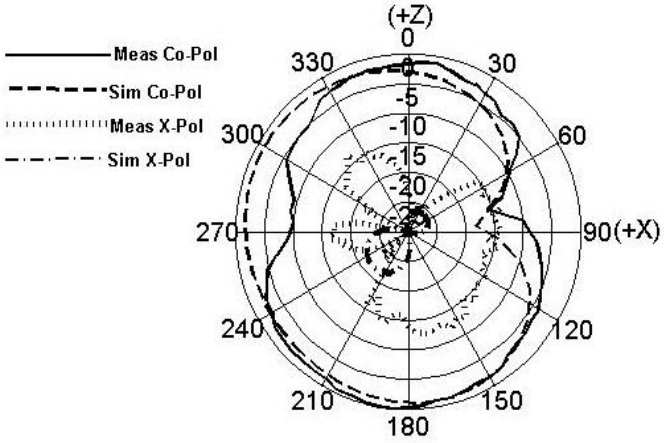

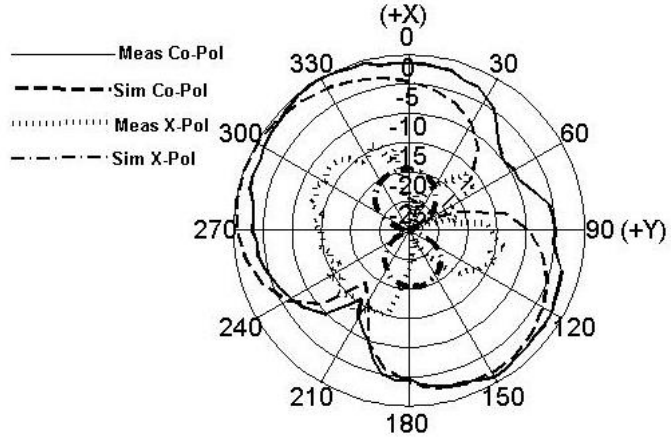

1.8 GHz

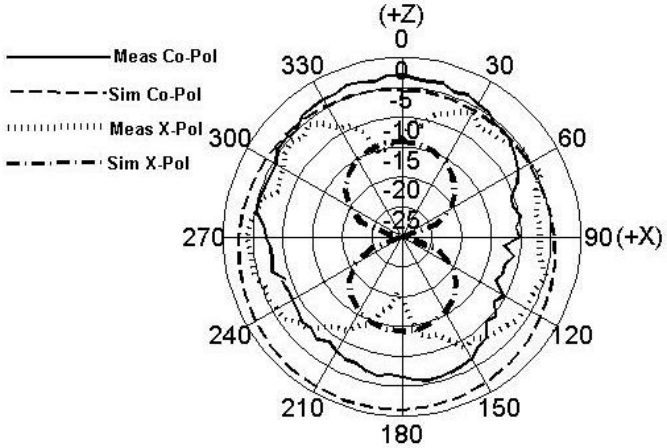

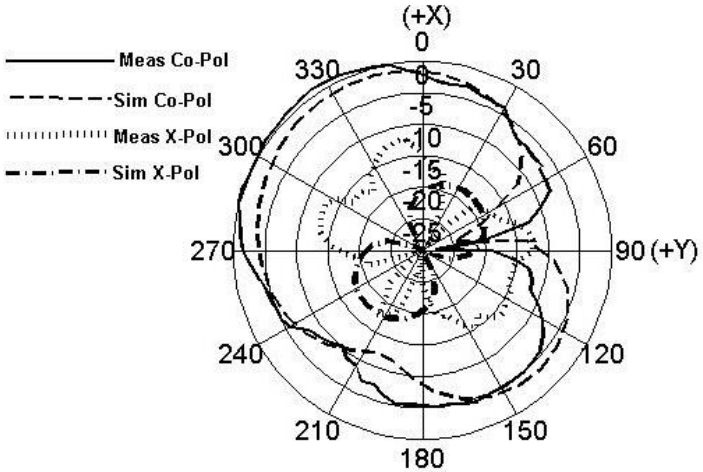

1.67 GHz

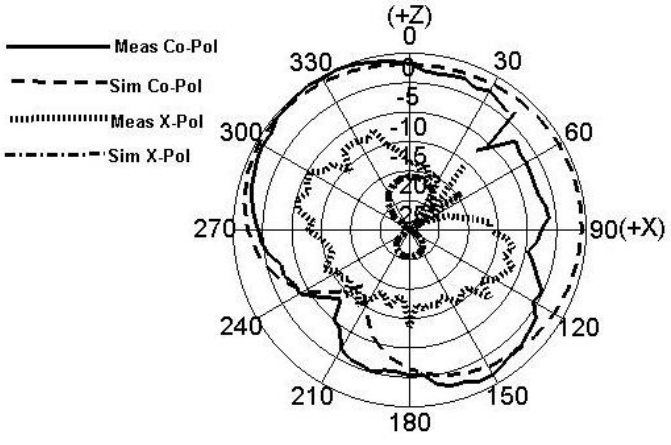

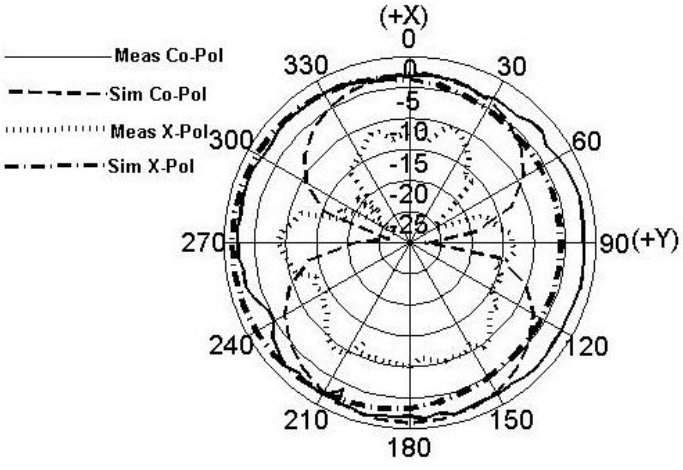

1.55 GHz

(a)

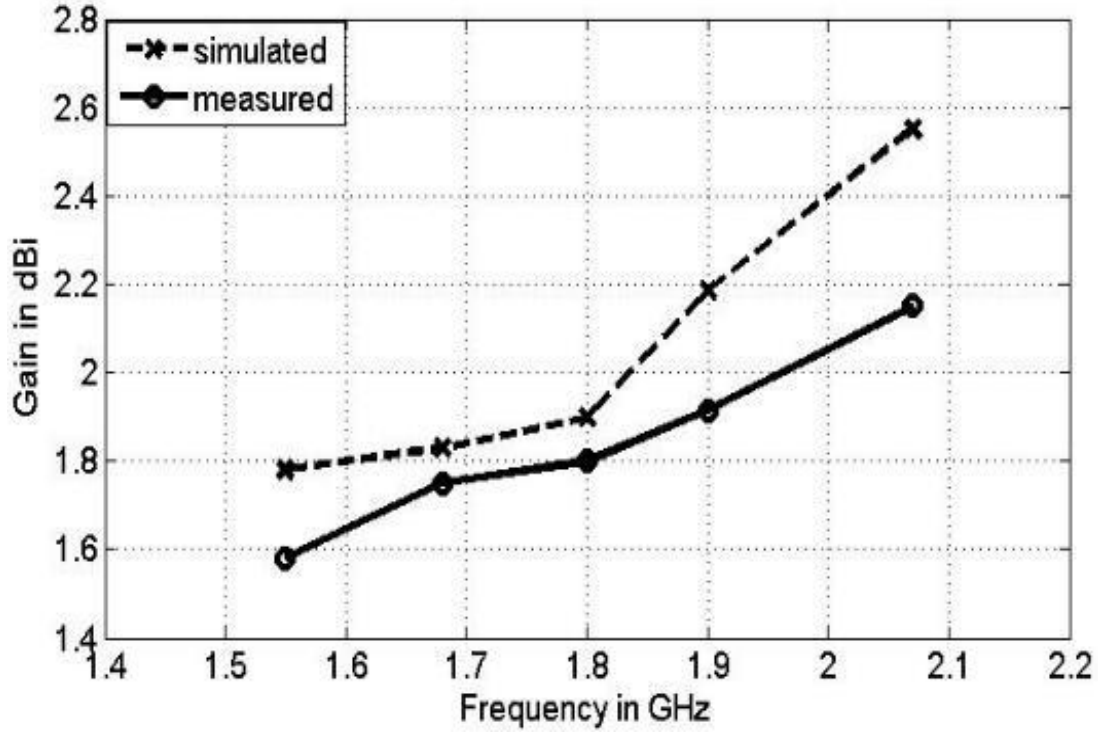

(b)

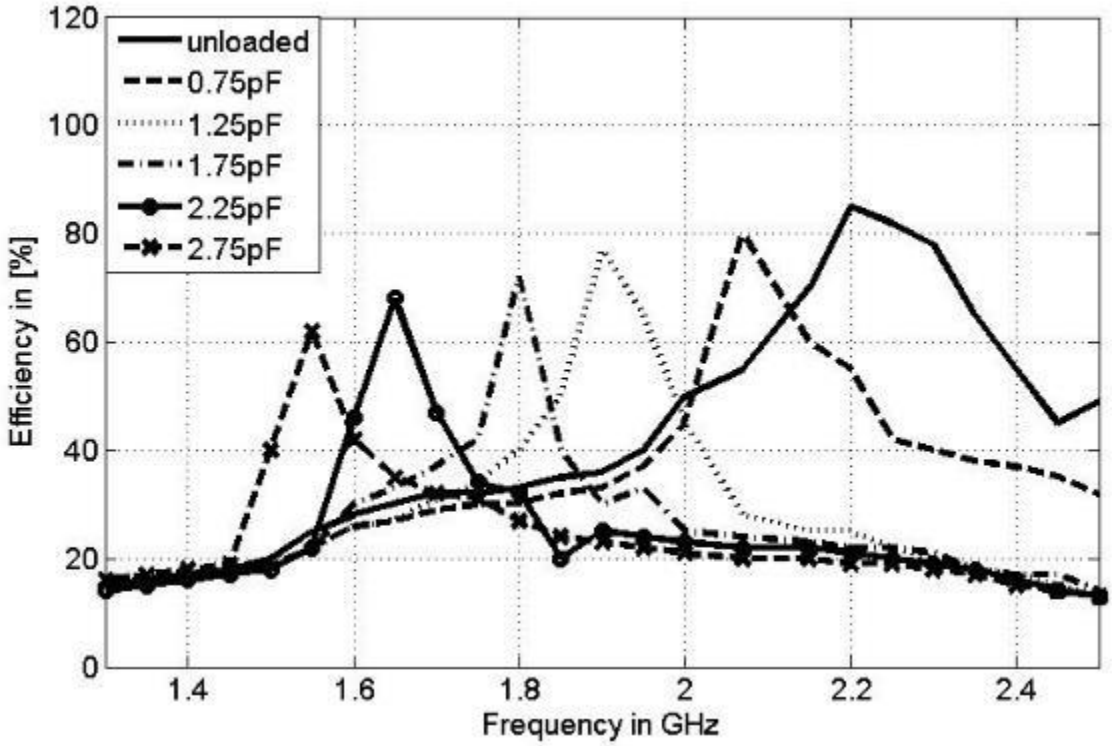

(c)

Figure 8: (a) Simulated against measured normalised antenna radiation patterns of the proposed loaded antenna for two planes (left: x-z plane, right: x-y plane) at 1.55, 1.67 1.8, 1.9 GHz and 2.07GHz, where port 1 (*left*) is excited and port 2 (*right*) is terminated in 50.

‘——’ measured co-polarisation.
‘– – –’ simulated co-polarisation
‘…….’ measured cross-polarisation
‘-------’ simulated cross-polarisation

(b) Simulated and Measured peak gain for proposed loaded MIMO antenna at 1.55, 1.67, 1.8, 1.9 GHz and 2.07GHz. (c) Radiation efficiency of proposed antenna.

Table I: The ECC and channel loss with bandwidth at each operating frequency band for the proposed design.

Loading Cap [pF]	Center Freq. [GHz]	Bandwidth [%]	Envelope Correlation Coefficient (ECC)	Channel Capacity Loss [bps/Hz]
0.75	2.07	8	0.01	0.24
1.25	1.9	10	0.005	0.25
1.75	1.8	9.5	0.006	0.23
2.25	1.67	7	0.01	0.24
2.75	1.55	6.5	0.008	0.23

Far-field radiation patterns of the prototype loaded MIMO antenna were measured in a far-field anechoic chamber. The reference antenna was a broadband horn (EMCO type 3115) positioned at 4 m from the antenna under test where the input port of antenna-1 is excited and input port of antenna-2 is terminated by 50 ohm load. Two pattern cuts (i.e. the *xz* and *xy* planes) were taken at 1.55, 1.67, 1.8, 1.9 and 2.07 GHz when the capacitance of the varactor diode was varied respectively: 0.75pF, 1.25pF, 1.75pF, 2.25pF and 2.75pF. The simulated patterns were generated from HFSS for the same cut planes. The patterns were normalized for ease of comparison and presented by Fig.8a. The results indicate a notable agreement between the simulated and measured radiation patterns at all the designated frequencies, as shown in Fig. 8a. Significantly, these radiation patterns are consistent over the operating bands. The results show that the radiation patterns are more or less omnidirectional.

Fig. 8b illustrates the measured loaded MIMO antenna gain compared with the simulations in the broadside direction for frequencies between 1550 and 2070 MHz as the capacitance value varied from 0.75pF to 2.75pF accordingly. It was found that the maximum measured antenna gain at the selected frequency bands were 1.58, 1.75, 1.8, 1.9, and 2.15 dBi, respectively, whereas the simulated gains were found to be 1.78, 1.83, 1.91, 2.18, and 2.55 dBi across the chosen frequency bands. There is a small discrepancy between the measured and simulated results. This may be accounted for by (1) misalignment of the capacitor in the antenna assembly, and (2) the fact that the presence of the SMA connector pin in the measurement was not taken into consideration in the modelling processes. Nonetheless, these results can be said to be in reasonable agreement.

The radiation efficiency of the proposed antenna is shown in Fig. 8c. These curves include the effect of the return power loss and inter-port coupling; in which the total efficiencies achieved on lower side but reasonable around the selected tuned bands. The antenna efficiency decreases from 82 % to 62 % when the capacitance value increases from 0.75pF to 2.75pF respectively. The efficiencies over the operating bands are reasonable for practical mobile and portable wireless applications.

4. CONCLUSION

A small-size tunable printed multiple-input and multiple output antenna has been presented. A ground plane with an I-shaped branch was used to reduce the mutual coupling between the antennas elements. This tunable MIMO antenna provides better than -13 dB mutual coupling covering the entire frequency band for a separation distance of 0.012 wavelength. The prototypes of the proposed unloaded and loaded MIMO antennas have been successfully

implemented and reasonable antenna performances were observed. By varying the capacitance value from 0.75pF to 2.75pF, the resonant frequency was shifted downwards from 2.07GHz to 1.55GHz whilst maintaining the return loss (S_{11}) below −10 dB and the isolation characteristic (S_{21}) less than −13dB. Both the simulated and the measured patterns are given in good agreement. Moreover, the envelope correlation coefficient of this MIMO antenna is well below 0.025 which leads to a good diversity characteristic to mitigate the multipath fading. The proposed design is simple and low cost providing a promising solution for mobile terminals such as PDA and tablet computers.

ACKNOWLEDGMENT

This work has been performed in the framework of ARTEMOS project under work programme ENIAC JU 2010 and FCT (Fundação para a Ciência e Tecnologia) .The authors would like to thank Datong PLC (Leeds LS18 4EG, West Yorkshire, U.K.), for their financial support of the Knowledge Transfer Partnership (KTP No: 008734).

References

[1] Y. Gao, X. Chen, Z. Ying, and C. Parini, “Design and Performance Investigation of a Dual-Element PIFA Array at 2.5 GHz for MIMO Terminal,” *IEEE Trans. Antennas Propag.*, vol. 55, no. 12, pp. 3433– 3441, Dec. 2007.

[2] Y. Ding, Z. Du, K. Gong, and Z. Feng, “ A Four-Element Antenna System for Mobile Phone,” *IEEE Antennas and Wireless Propagation Letters*, Vol. 6, pp. 655-658, 2007.

[3] C.H. See, R.A. Abd-Alhameed, Z.Z. Abidin, N.J. McEwan and P.S. Excell, “Wideband Printed MIMO/Diversity Monopole Antenna for WiFi/WiMAX Applications,” *IEEE Trans. Antennas Propag.*, vol.60, no.4, pp.2028-2035, April 2012.

[4] L. Xiong and P. Gao “Compact Dual-Band Printed Diversity Antenna for WIMAX/WLAN Applications,” *Progress In Electromagnetics Research C*, Vol. 32, 151-165, 2012.

[5] S. M. A. Nezhad and H.R. Hassani, "A Novel Tri-Band E-shaped Printed Monopole Antenna for MIMO Application," *IEEE Antennas and Wireless Propagation Letters*, Vol. 9, pp.576-579, 2010

[6] G. J. Foschini and M. J. Gans, “On Limits of Wireless Communications In a Fading Environment When Using Multiple Antennas,” *Wireless Personal Communications*, vol. 6, no. 3, pp. 311– 335, 1998.

[7] Y. Gao, X. Chen, Z. Ying, and C. Parini, “Design and Performance Investigation of a Dual-Element PIFA Array at 2.5 GHz for MIMO Terminal,” *IEEE Trans. Antennas Propag.*, vol. 55, no. 12, pp. 3433–3441, 2007.

[8] D. Pozar, “Input Impedance and Mutual Coupling of Rectangular Microstrip Antennas,” *IEEE Trans. Antennas Propag.*, vol. AP–30, pp. 1191–1196, Nov. 1982.

[9] A. Derneryd and G. Kristensson, “Signal Correlation Including Antenna Coupling,” *Electronics Letters*, vol. 40, no. 3, pp. 157– 159, 2004.

[10] M. Karakoikis, C. Soras, G. Tsachtsiris, and V. Makios, "Compact Dual-Printed Inverted-F Antenna Diversity Systems for Portable Wireless Devices," *IEEE Antennas and Wireless Propagation Letters*, vol. 3, no. 1, pp. 9–14, 2004.

[11] Y. Ding, Z. Du, K. Gong, and Z. Feng, "A Novel Dual-Band Printed Diversity Antenna for Mobile Terminals," *IEEE Trans. Antennas Propag.*, vol. 55, no. 7, pp. 2088–2096, 2007.

[12] Kin-Lu Wong, Ting-Wei Kang, and Ming-Fang Tu " Internal Mobile Phone Antenna Array for LTE/WWAN and LTE MIMO Operations" *Microwave and Optical Technology Letters*, Vol. 53, No. 7, pp. 1596-1573. July 2011

[13] S.C. Chen, Y.S.Wang, and S. J. Chung, "A Decoupling Technique for Increasing the Port Isolation Between Two Strongly Coupled Antennas," *IEEE Trans. Antennas Propag.*, vol. 56, no. 12, pp. 3650–3658, Dec. 2008.

[14] D. Sievenpiper, L. Zhang, R. F. J. Broas, N. G. Alexopolus, and E. Yablonovitch, "High-Impedance Electromagnetic Surfaces with a Forbidden Frequency Band," *IEEE Trans. Microw. Theory Tech.*, vol. 47, pp. 2059–2074, 1999.

[15] F. Yang and Y. Rahmat-Samii, "Microstrip Antennas Integrated with Electromagnetic Band-Gap (EBG) Structures: A low mutual coupling design for array applications," *IEEE Trans. Antennas Propag.*, vol. 51, no. 10, pp. 2936–2946, Oct. 2003.

[16] G. Dadashzadeh, A. Dadgarpour, F. Jolani, and B. S. Virdee, "Mutual Coupling Suppression in Slosely Spaced Antennas," *IET Microw. Antennas Propag.*, vol. 5, no. 1, pp. 113–125, Jan. 12, 2011.

[17] Z. Z. Abidin, R. A. Abd-Alhameed, N. McEwan, S. M. R. Jones, K. N. Ramli, and A. Alhaddad, "Design and analysis of UC-EBG on Mutual Coupling Reduction," *The Proceeding of Loughborough Antennas & Propagation Conference*, pp. 693-696, November 2009.

[18] Z. Z. Abidin, Y. Ma, R. A. Abd-Alhameed, K. N. Ramli, D. Zhou, M. S. Bin-Melha, J. M. Noras, and R. Halliwell "Design of 2 x 2 U-shape MIMO slot antennas with EBG material for mobile handset applications" *Progress In Electromagnetics Research Symposium Proceedings*, Marrakesh, Morocco, Mar, 2011.pp.1275-1978.

[19] A. Diallo, C. Luxey, P. L. Thuc, R. Staraj, and G. Kossiavas, "Enhanced Two-Antenna Structures for Universal Mobile Telecommunications System Diversity Terminals," *IET Microw. Antennas Propag.*, vol. 2, no. 1, pp. 93–101, Feb. 2008.

[20] A. Chebihi, C. Luxey, A. Diallo, P. L. Thuc, and R. Staraj, "A novel Isolation Technique for Closely Spaced PIFAs for UMTS Mobile Phones," *IEEE Antennas Wireless Propag. Lett.*, vol. 7, pp. 665–668, 2008.

[21] Z. Li, K. Ito, Z. Du, and K. Gong, "Compact Wideband Printed Diversity Antenna for Mobile Handsets," *in Proc. Asia–Pac. Radio Sci. Conf.,* Toyama, Japan, pp. 1–4, Oct. 2010

[22] A. Diallo, C. Luxey, P. L. Thuc, R. Staraj, and G. Kossiavas, "Study and Reduction of the Mutual Coupling Between Two Mobile Phone PIFAs Operating in the DCS1800 and UMTS Bands," *IEEE Trans. Antennas Propag*., vol. 54, no. 11, pp. 3063–3074, Nov. 2006.

[23] S.W. Su, C.T. Lee, and F.S. Chang" Printed MIMO-Antenna System Using Neutralization-Line Technique for Wireless USB-Dongle Applications" *IEEE Trans. Antennas Propag*., vol. 60, no. 2, pp.456-463, Feb 2012.

[24] Y. Lee, D. Ga, and J. Choi "Design of a MIMO Antenna with Improved Isolation Using MNG Metamaterial", *International Journal of Antennas and Propagation*, Vol. 2012, pp.1-8, 2012.

[25] L.J. Chu, "Physical Limitations of Omnidirectional Antenna," *J. Appl. Phys*., Vol.19, pp. 163-1175, 1948

[26] D. Piazza, N. Kirsch, A. Forenza, R. Heath, and K. Dandekar, "Design and Evaluation of a Reconfigurable Antenna Array for MIMO systems," *IEEE Trans. Antennas Propag.*, vol. 56, pp. 869 – 881, March 2008.

[27] M.I. Lai and S.K. Jeng, "Compact Pattern Reconfigurable Antenna Array Based on L-Shaped Slots and PIN Diodes for Adaptive MIMO Systems," *Antennas and Propagation Society International Symposium*, 2008. AP-S 2008. IEEE, pp. 1–4, 2008.

[28] Y. Cai and Z. Du, "A Novel Pattern Reconfigurable Aantenna Array for Diversity Systems," *IEEE Antennas and Wireless Propagation Letters*, vol. 8, pp. 1227 – 1230, 2009.

[29] B. A. Cetiner, E. Aksay, E. Sengul, and E. Ayanoglu, "A MIMOsystem with Multifunctional Reconfigurable Antenna," *IEEE Antennas and Wireless Propag. Lett.*, vol.5, pp. 463-466, 2006.

[30] J. Villanen, P. Suvikunnas, C. Icheln, J. Ollikainen, and P. Vainikainen, "Advances in Diversity Performance Analysis of Mobile Terminal Antennas," *in Proceedings of the*

International Symposium on Antennas and Propagation (ISAP '04), Sendai, Japan, August 2004.

[31] F.Y .Zulki, E. T. Rahardjo,"Compact MIMO Microstrip Antenna with Defected Ground for Mutual Coupling Suppression", *PIERS Draft Proceedings*, Marrakesh, MOROCCO, p. 94, March 20-23, 2011.

[32] R. Sadeghi Fakhr, A. A. L. Neyestanak, M. N. Moghaddasi, "Compact Size and Dual Band Semicircle Shaped Antenna for MIMO Applications", *Progress In Electromagnetics Research C*, vol. 11, pp. 147-154, 2009.

[33] K. Chung, J. H. Yoon ,"Integrated MIMO Antenna with High Isolation Characteristic" *Electron. Lett.*, vol. 43, pp. 199-201, 2007

[34] I.T.E. Elfergani, T. Sadeghpour, R.A. Abd-Alhameed, A.S. Hussaini, J.M. Noras S.M.R. Jones and J. Rodriguez, "Reconfigurable Antenna Design for Mobile Handsets Including Harmonic Radiation Measurements", *IET Microwaves, Antennas & Propagation*, Vol. 6, Iss. 9, pp. 990–999, July 2012

[35] I.T. E. Elfergani, R.A. Abd-Alhameed, C.H. See, T. Sadeghpour, J.M. Noras and S.M. R. Jones, "Small Size Tunable Printed F-Slot Antenna for Mobile Handset Applications ", *Microwave and Optical Technology Letters*, Vol. 54, No. 3, pp. 794-802. March 2012.

[36] High Frequency Structure Simulator (HFSS) v10 User's Guide, Ansoft Corp., Pittsburgh, PA, USA.

[37] A. C. K. Mak, C. R. Rowell, and R. D. Murch, "Isolation Enhancement Between Two Closely Packed Antennas," *IEEE Trans. Antennas Propag.*, vol. 56, no. 11, pp. 3411–3419, 2008.

[38] H. Chung, Y. Jang, and J. Choi, "Design of a Multiband Internal Antenna for Mobile Application," *in Proceedings of the IEEE International Symposium on Antennas and Propagation and USNC/URSI National Radio Science Meeting (APSURSI '09)*, pp. 1–4, June 2009.

[39] I. Salonen and P. Vainikainen, "Estimation of Signal Correlation in Antenna Arrays," *in Proceedings of the 12th International Symposium Antennas*, vol. 2, pp. 383–386, July 2002.

[40] S. Blanch, J. Romeu, and I. Corbella, "Exact Representation of Antenna System Diversity Performance from Input Parameter Description," *Electronics Letters*, vol. 39, no. 9, pp. 705–707, 2003.

[41] S. H. Chae, S.-K. Oh, and S.-O. Park, “Analysis of Mutual Coupling, Correlations, and TARC in WiBro MIMO Array Antenna,” *IEEE Antenna Propag. Lett.*, vol. 6, pp. 122–125, 2007.

[42] D. Valderas, P. Crespo, and C. Ling, “UWB Portable Printed Monopole Array Design for MIMO Communications,” *Microw. Opt. Technol. Lett.*, vol. 52, no. 4, pp. 889–895, 2010.